

Coordinated microRNA/mRNA expression profiles reveal a putative mechanism of corneal epithelial cell transdifferentiation from skin epidermal stem cells

YANJIIE GUO, XIYA MA, WEINI WU, MINGYAN SHI, JUNLONG MA, YAPING ZHANG, ERKANG ZHAO and XUEYI YANG

Life Science College, Luoyang Normal University, Luoyang, Henan 471934, P.R. China

Received November 16, 2016; Accepted November 15, 2017

DOI: 10.3892/ijmm.2017.3304

Abstract. Skin epidermal stem cells (SESCs), which share a single origin with corneal epithelial cells (CECs), are considered to be one of the most ideal seed cells for the construction of tissue engineered corneas. However, the mechanism underlying the transdifferentiation of SESC to CECs has not been fully elucidated. In the present study, to identify critical microRNAs (miRNAs/miRs) and genes that regulate the transdifferentiation of SESC to CECs, SESC and CECs were collected from sheep and used for small RNA sequencing and mRNA microarray analyses. Among the differentially expressed miRNAs and genes, 36 miRNAs were downregulated and 123 genes were upregulated in the CECs compared with those in the SESC. miR-10b exhibited the largest change in expression between the cell types. Target genes of the 36 downregulated miRNAs were predicted and a computational approach demonstrated that these target genes may be involved in several signaling pathways, including the 'PI3K signaling pathway', the 'Wnt signaling pathway' and the 'MAPK signaling pathway', as well as in 'focal adhesion'. Comparison of these target genes to the 123 upregulated genes identified 43 intersection genes. A regulatory network of these 43 intersection genes and its correlative miRNAs were constructed, and three genes (dedicator of cytokinesis 9, neuronal differentiation 1 and activated leukocyte cell adhesion molecule) were found to have high interaction frequencies. The expression levels of 7 randomly selected miRNAs and the 3 intersection genes were further validated by reverse transcription-quantitative polymerase chain reaction. It was found that miR-10b, the Wnt signaling pathway and the 3 intersection

genes may act together and serve a critical role in the transdifferentiation process. This study identified miRNAs and genes that were expressed in SESC and CECs that may assist in uncovering its underlying molecular mechanism, as well as promote corneal tissue engineering using epidermal stem cells for clinical applications.

Introduction

The corneal epithelium (CE) is the exfoliated multilayer epithelium that forms the anterior surface layer of the cornea (1). Corneal epithelial cell (CEC) homeostasis is a requirement for both ocular surface integrity and corneal transparency and visual function (2). Corneal damage, including infection, trauma and denaturation, have severe consequences for the ocular surface, which in turn may affect the integrity of the CE and visual function, ultimately leading to functional blindness (3). There were approximately 4.9-10 million people with corneal blindness worldwide in 2012 (4). One of the most successful strategies for ocular surface reconstruction is the transplantation of epithelial cell sheets engineered from autologous limbal epithelial cells (1,5,6); it is effective in animal models and humans. However, a limbal biopsy is required for the isolation of limbal epithelial cells, which may pose a risk to the contralateral healthy eye and is not useful for treating bilateral limbal stem cell deficiency. Allogeneic limbal epithelium transplantation (7), one optional treatment, has limitations of immunological rejection, donor scarcity and an extremely low long-term success rate. Thus, it is reasonable to find and evaluate alternative autologous stem cell sources for *in vitro* culture and transplantation to avoid the risk of immunological rejection and to satisfy the demand from patients with corneal blindness.

Other cell sources, including oral mucosal epithelial cells (8-10), mesenchymal stem cells (11,12), embryonic stem cells (13) and immature dental pulp stem cells (14), have been established for corneal epithelium replacement, but to date, no long-term results have been reported or achieved. Stem cells residing within the epidermis have the potential of multi-directional differentiation. In addition to differentiating into skin cells and appendages, skin epidermal stem cells (SESCs) can differentiate into other lineages, including

Correspondence to: Professor Xueyi Yang, Life Science College, Luoyang Normal University, 6 Jiqing Road, Luoyang, Henan 471934, P.R. China
E-mail: yangxueyi2002@aliyun.com

Key words: skin epidermal stem cells, microRNAs, corneal epithelia, microarray

nerve cells (15) and germ cells (16). Moreover, SESCOs and limbal stem cells are of the same origin, namely, the basal layer of embryonic skin, and are thus keratinocyte stem cells (17,18), which express specific types of cytokeratin protein (K1, K3, K5, K10, K12, K14, K15 and K19) on their surfaces (19-21). It is hypothesized that SESCOs are ideal seed cells that may be utilized to replace limbal stem cells for tissue engineered cornea construction. There have been certain attempts to use hair follicle stem cells (22) and skin-derived precursor cells (2,23); however, the mechanisms involved, particularly the regulatory role of miRNAs in this process, have not been fully elucidated. In the present study, the expression profile of microRNAs (miRNAs/miRs) was compared in the SESCOs and CECs of sheep. The findings of this study may be useful in the elucidation of the mechanisms underlying the molecular regulation of the transdifferentiation process of SESCOs into CECs.

Materials and methods

Cells. SESCOs and CECs were obtained from 2 male small-tailed Han sheep (obtained from the Experimental Animal Center of Shaanxi Center for Stem Cell Engineering and Technology, Northwest A&F University) following a protocol approved by the Medical Animal Care and Welfare Committee of Luoyang Normal University. The isolation of CECs and SESCOs were performed as previously described (24,25).

Small RNA sequencing. Total RNA (3 μ g) from the SESCOs and CECs was used as input material for the generation of small RNA libraries. Sequencing libraries were generated using the NEBNext[®] Multiplex Small RNA Library Prep Set for Illumina[®] (New England Biolabs, Inc., Ipswich, MA, USA) following the manufacturer's instructions, and index codes were added to attribute sequences to each sample. The clustering of the index-coded samples was performed on a cBot Cluster Generation System using TruSeq SR Cluster kit v3-cBot-HS (Illumina, Inc., San Diego, CA, USA), according to the manufacturer's instructions. Following cluster generation, the library preparations were sequenced on an Illumina HiSeq 2500/2000 platform (Illumina, Inc.) and 50-bp single-end reads were generated.

The raw sequence reads were first trimmed from the adapter sequence using a Perl script and adapter-trimmed reads longer than 18 nt were used for further analysis as clean reads. To further parse the clean reads, the Integrative Short Reads Navigator software (freely accessed at <http://omicslab.genetics.ac.cn/ISRNA/>) was used based on the manufacturer's instructions. Bowtie software (version 1.1.2, open-source software maintained by Johns Hopkins University) was used to map sequences to sheep genomes (*Ovis aries*). Annotation of the short sequence reads was performed using the BLAST + program (<ftp://ftp.ncbi.nlm.nih.gov/blast/executables/blast+/LATEST/>) and the Rfam database (<http://rfam.xfam.org/>). Known miRNA sequences were extracted from miRBase (<http://www.mirbase.org/>). The frequency of miRNA reads was normalized as transcripts per million, then the normalized expression levels of miRNAs between two samples were conducted to calculate fold-changes. The identification of differentially expressed miRNAs between

two different samples was performed based on the \log_{10} ratio of fold-changes. Hierarchical clustering was performed using Heatmap.2 (R language gplots package). The levels of miRNA expression were clustered using average linkage clustering. The average value of the distance of each miRNA was used to measure cluster-to-cluster distance.

mRNA microarray analysis. The transcriptional profiles of the SESCOs and CECs were analyzed. Total RNA was extracted and purified using the miRNeasy mini kit (Qiagen GmbH, Hilden, Germany) following the manufacturer's instructions and an RIN number was checked for to determine RNA integrity using an Agilent Bioanalyzer 2100 (Agilent Technologies, Inc., Santa Clara, CA, USA). Total RNA was amplified and labeled using a Low Input Quick Amp Labeling kit, One-Color (Agilent Technologies, Inc.), following the manufacturer's instructions. Labeled cRNAs were purified using an RNeasy mini kit (Qiagen GmbH). Each slide was hybridized with 600 ng Cy3-labeled cRNA using a gene expression hybridization kit in a hybridization oven (both Agilent Technologies, Inc.), according to the manufacturer's instructions. After 17 h of hybridization, slides were washed in staining dishes (Thermo Fisher Scientific, Inc., Waltham, MA, USA) with a gene expression wash buffer kit (Agilent Technologies, Inc.), following the manufacturer's instructions. Slides were scanned on a Agilent Microarray Scanner (Agilent Technologies) using the following default settings: Dye channel, green; scan resolution, 5 μ m; PMT, 100 and 10%, 16-bit. Data were extracted using Feature Extraction 10.7 (Agilent Technologies, Inc.). Raw data were normalized using a Quantile algorithm, Gene Spring Software 11.0 (Agilent Technologies, Inc.).

Target prediction and network construction. As there was no appropriate database or methods for predicting sheep miRNA target genes, the human orthologs of differentially expressed sheep miRNA sequences were used to identify potential target genes by searching the TargetScan database (http://www.targetscan.org/vert_71/). JAVA (version 1.8.0_101; Oracle Software Systems Ltd., Redwood Shore, CA, USA) and Cytoscape 2.6.0 (version 2.6.0, open-source software) software were used to construct regulatory miRNA-target gene networks based on regulatory interactions between differentially expressed miRNAs.

Gene Ontology (GO) and Kyoto Encyclopedia of Genes and Genomes (KEGG) pathway analyses. GO (<http://geneontology.org/>) and KEGG (<http://www.kegg.jp/>) pathway analyses of differentially expressed genes were performed using the Database for Annotation, Visualization and Integrated Discovery (DAVID; <https://david.ncifcrf.gov/>); a hypergeometric test with the Benjamini and Hochberg false discovery rate (FDR) was performed using the default parameters to adjust the P-value. A bubble chart was plotted using the OmicShare tools, a free online platform for data analysis (www.omicshare.com/tools).

Reverse transcription-quantitative polymerase chain reaction (RT-qPCR). RT-qPCR was performed to validate the expression levels of the analyzed miRNAs by sequencing. Reverse transcription was performed in a 20- μ l reaction containing

Table I. Statistics based on the reads of the sequencing data.

Reads	Corneal epithelial cell count	Skin epidermal stem cell count
Raw reads	13,708,257	14,358,739
Clean reads	13,485,770	14,152,453
Annotated reads	11,289,227	11,969,113
with miRBase	5,774,859	6,283,880
with piRNA	127,061	155,238
with Rfam v.10	4,520,579	4,752,923
with ncRNA	866,728	777,072
Unannotated reads	2,196,543	2,183,340
Novel miRNA	832,45	853,42

miRNA, microRNA.

2 μ l total RNA, 1 μ l of 5 μ M RT primer, 1 μ l of 10 mM dNTPs, 4 μ l 5X PrimeScript buffer and 200 units of PrimeScript RTase (Takara Bio, Inc., Otsu, Japan). The primers used were as follows: U6 forward, 5'-CTCGCTTCGGCAGCACCA-3' and reverse, 5'-AACGCTTCACGAATTTGCGT-3'; miR-127 forward, 5'-ACACTCCAGCTGGGCTGAAGCTCAGAGGG-3'; miR-376c forward, 5'-ACACTCCAGCTGGGAACA TAGAGGAAA-3'; miR-382 forward, 5'-ACACTCCAGCTG GGAATCATTACGGAC-3'; miR-758 forward, 5'-ACA CTCCAGCTGGGTTTGTGACCTGGTC-3'; miR-154 forward, 5'-ACACTCCAGCTGGGTAGGTTATCCGT GTTG-3'; miR-409 forward, 5'-ACACTCCAGCTGGGGAA TGTGCTCGGTG-3'; miR-10b forward, 5'-ACACTCCA GCTGGGTACCCTGTAGAACCGAA-3' (all miRs had the same reverse primer, 5'-TGGTGTCGTGGAGTCG-3'); DOCK9 forward, 5'-TTAAGGATGCATCTGGAAACC-3' and reverse, 5'-CTTGAGCATGTCTTCATTGGA-3'; NEUROD1 forward, 5'-CTTCGATAGCCATTCACATCAT-3' and reverse, 5'-TGAAACTGACGTGCCTCTAATC-3'; ALCAM forward, 5'-CTTCAGCAGCCATCACAGTT-3' and reverse, 5'-AGAGCATCGCCTATCTGCTT-3'; GAPDH forward, 5'-CTGGCCAAGGTCATCCAT-3' and reverse, 5'-ACAGTCTTCTGGGTGGCAGT-3'. The reaction was incubated at 42°C for 60 min, and then terminated by heating at 85°C for 5 min. The qPCR amplification was performed using SYBR-Green I® (Roche Diagnostics, Indianapolis, IN, USA). The reactions were performed for 35 cycles at 94°C for 30 sec, 54-60°C for 30 sec, and 72°C for 30 sec. All reactions were run in triplicate. U6 small nuclear RNA was used as an internal reference control, and the data were analyzed using the $2^{-\Delta\Delta Ct}$ method (26).

Statistical analysis. Data were analyzed using SPSS software (version 22.0; SPSS, Inc., Chicago, IL, USA). All measurement data are presented as the mean \pm standard deviation. Statistical significance analysis of involved measurement data was performed using paired Student's t-tests. $P < 0.05$ was considered to indicate a statistically significant difference.

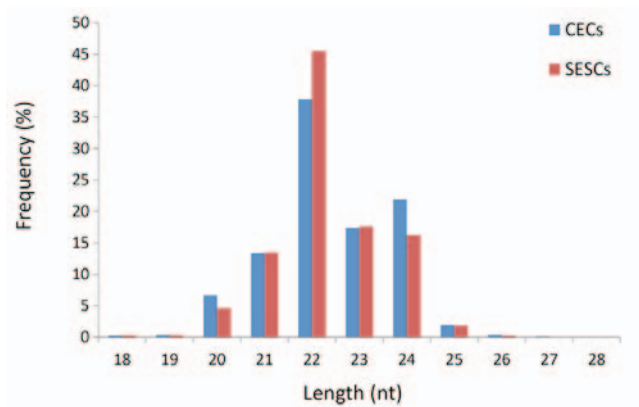


Figure 1. Size and frequency distribution of the sequencing reads. nt, nucleotides; CECs, corneal epithelial cells; SESC, skin epidermal stem cells.

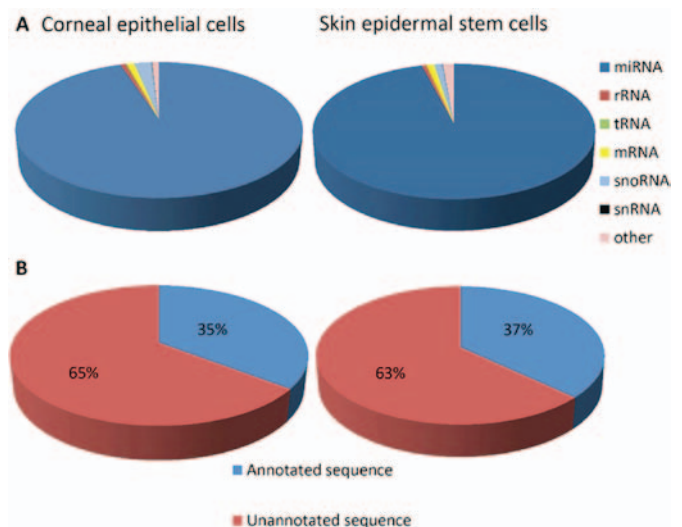


Figure 2. Composition of small RNA classes of the sequencing results. (A) Different types of small RNA represented in CECs and SESC. (B) Frequency of annotated and unannotated sequences in CECs and SESC. CECs, corneal epithelial cells; SESC, skin epidermal stem cells; miRNA, microRNA.

Results

Overview of small RNA sequencing data. To identify differentially expressed miRNAs in the SESC and CECs of sheep, two small RNA libraries were constructed by deep sequencing. The results of 14.36 million (M) and 13.71 M total reads were obtained from the cell libraries of SESC and CECs, respectively. Subsequent to removing the low-quality and adaptor sequences, a total of 14.15 and 13.48 M clean reads were ultimately obtained. Subsequently, all identical sequence reads were classified as groups, and 0.21 and 0.22 M unique sequences associated with individual sequence reads, respectively, were obtained (Table I). The size distribution of the reads was similar between the two libraries (Fig. 1). The majority of the small RNAs were 21-24 nt in size. Sequences 22 nt in length, the typical size of Dicer-derived products, accounted for 45.47 and 35.85% of the total sequence reads in the SESC and CEC libraries, respectively. The composition of the RNA classes in each library is shown in Fig. 2A. Conserved

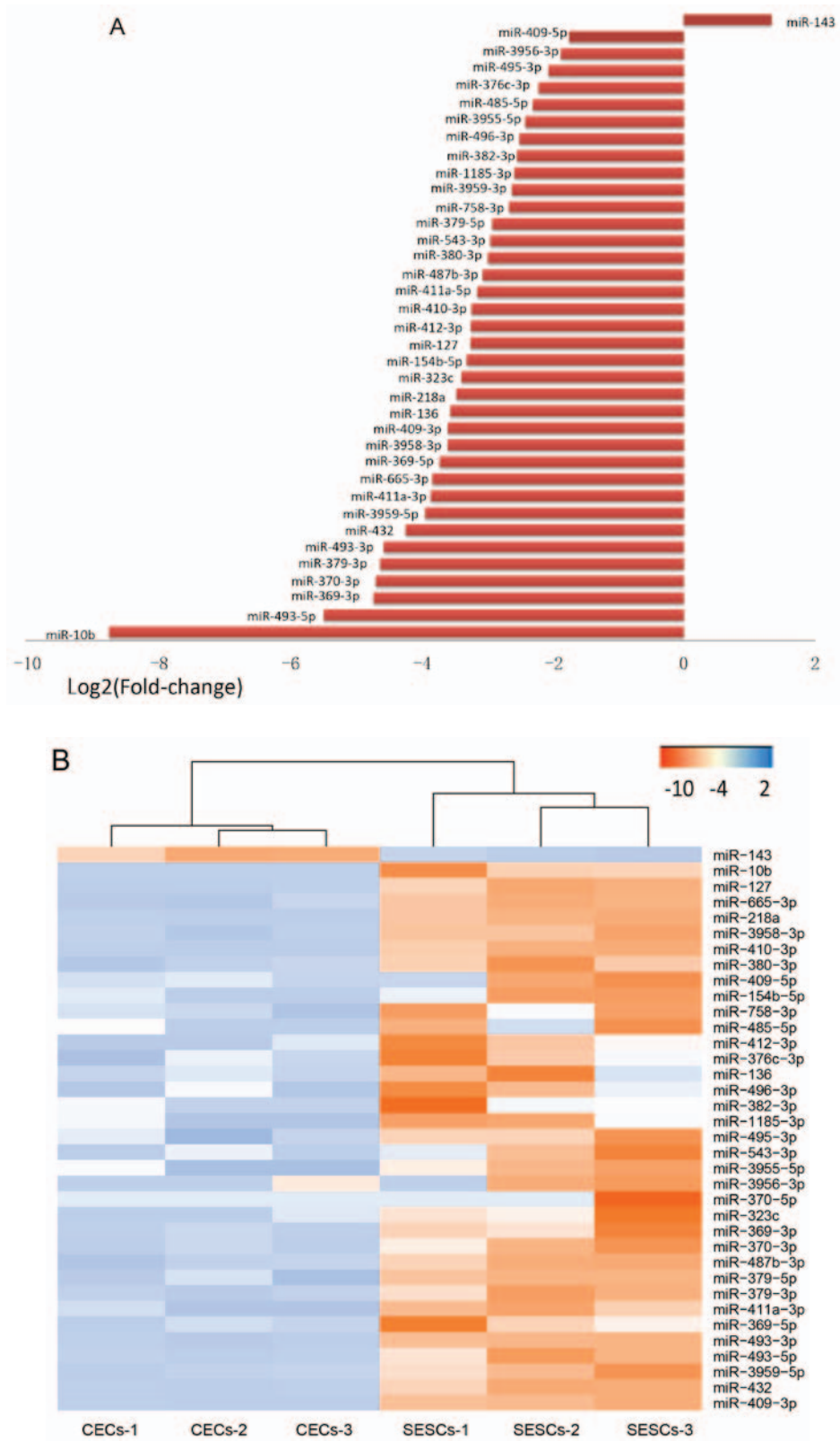


Figure 3. miRNA profiles were assessed between CECs and SESC. (A) Fold-change (ratio between CECs/SESCs) in miRNA expression between the CECs and SESC. miR-10b exhibited the greatest increase in expression in SESC. (B) Hierarchical clustering was performed with normalized miRNA data (fold-change >2). A total of 36 miRNAs were identified whose expression was significantly altered in the CECs and SESC. CECs, corneal epithelial cells; SESC, skin epidermal stem cells; miR/miRNA, microRNA.

miRNAs accounted for 95.88 and 95.01% of the total sequence reads (Fig. 2A) in the SESC and CEC small RNA libraries, respectively. The detection of a low proportion of long RNAs, including mRNA (1.02 and 1.03%), rRNA (0.54 and 0.63%) and

snoRNA (1.06 and 2.32%) (Fig. 2A), in the respective SESC and CEC small RNA libraries indicated that the samples were not contaminated by degraded RNA. In addition, the highest fraction of unique reads (63 and 65% in the SESC and CEC libraries,

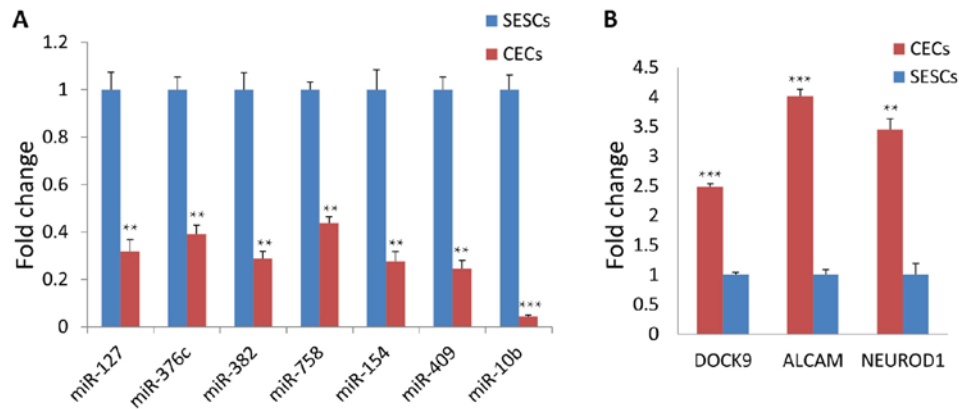


Figure 4. Validation of selected miRNAs and mRNAs by reverse transcription-quantitative polymerase chain reaction. (A) The results showed that the expression of miR-127, 376c, 382, 758, 154, 409 and 10b was markedly downregulated in CECs compared with that in SESC. (B) Meanwhile, DOCK9, ALCAM and NEUROD1 expression was upregulated in CECs compared with that in SESC. CECs, corneal epithelial cells; SESC, skin epidermal stem cells; miR/miRNA, microRNA; DOCK9, dedicator of cytokinesis 9; NEUROD1, neuronal differentiation 1; ALCAM, activated leukocyte cell adhesion molecule.

respectively) was attributed to unannotated sequences (Fig. 2B). A total of 136 and 94 conserved miRNAs were identified in the SESC and CEC libraries, respectively; 184 and 169 miRNAs were mapped to the sheep genome, with the extended genome sequences having the potential to form hairpins.

Differential expression of miRNAs and mRNA in SESC and CECs. To identify miRNAs that may be involved in the transdifferentiation process of SESC to CECs, the miRNA and mRNA expression profiles were assessed in these two cells using small RNA deep sequencing and microarray analysis, respectively. The threshold used to screen upregulated or downregulated miRNAs and mRNAs was a fold-change of ≥ 2.0 . A total of 37 miRNAs were found to be differentially expressed (Fig. 3). Among these miRNAs, 36 were found to be downregulated by < 0.5 -fold, and 1 (miR-143) was found to be upregulated > 2.0 -fold in SESC compared with that in CECs (Fig. 3A). The fold-change of downregulated miRNAs ranged from -425.71 to -3.34, and miR-10b exhibited the greatest decrease in expression in SESC compared with CECs. Hierarchical clustering was performed with normalized miRNA data (fold-change > 2). A total of 37 miRNAs were identified whose expression was significantly altered in the CECs and SESC (Fig. 3B). Differential expressions of miRNAs and mRNAs were identified as those meeting the criteria of FDR < 0.05 and \log_2 FoldChange > 1 .

A total of 241 mRNAs were found to be differentially expressed. Among these mRNAs, 123 were downregulated by < 0.5 -fold and 118 were upregulated by > 2.0 -fold in SESC compared with that in CECs. The fold-change ranged from -62.50 to -2.02 and from 2.00 to 155.76 for the downregulated and upregulated genes in SESC compared with that in CECs, respectively.

RT-qPCR confirmation of differential miRNA expression. A total of 7 differentially expressed miRNAs (Fig. 4) were randomly chosen for validation by RT-qPCR using the same RNA samples that were applied to the small RNA sequencing. The expression levels of all 7 miRNAs determined by RT-qPCR were concordant with their small RNA sequencing data (Fig. 4), indicating a strong association between miRNA profiling and the RT-qPCR data.

Target prediction and functional analysis of differentially expressed miRNAs. As aforementioned, 36 miRNAs were found to be downregulated in the SESC compared those in the CECs, and candidate target genes for all downregulated miRNAs were identified using the commonly used prediction algorithm, TargetScan. These targets were sorted by the enrichment of GO categories based on DAVID and mainly clustered into different functional groups (Fig. 5A). Targets were then functionally analyzed using the KEGG pathways database. Pathway analyses showed that these target genes were apparently associated with several pathways, including the 'PI3K-Akt signaling pathway', the 'Wnt signaling pathway', 'focal adhesion', the 'ErbB signaling pathway' and the 'MAPK signaling pathway' (Fig. 5B).

Intersection genes between differentially expressed miRNA target genes and differentially expressed genes. As previously described, a total of 9,660 genes were predicted by TargetScan for 36 downregulated miRNAs, and microarray analysis determined that 123 genes were expressed at higher levels in CECs than in SESC. These two set of genes were compared and 43 intersection genes were detected. Notably, 24 miRNAs of the 36 downregulated miRNAs were associated with these 43 intersection genes. These findings suggested that these miRNAs likely regulate the same biological process.

Function analysis of differentially expressed miRNA target genes and intersection genes

GO enrichment and KEGG pathway analyses. The intersection genes were sorted by the enrichment of GO categories based on DAVID and mainly clustered into different functional groups (Fig. 6A), and then were functionally analyzed using the KEGG pathways database. Fig. 6B shows 10 of the most significant pathways.

Construction of a regulatory and interaction network. A regulatory network was performed using the differentially expressed miRNAs and its target genes (Fig. 7). As previously described, 24 miRNAs of the 36 downregulated miRNAs were associated with these 43 intersection genes. A regulatory network of these 24 miRNAs and 43 intersection genes was then constructed using Cytoscape (Fig. 8). It was observed that dedicator of cytokinesis 9 (DOCK9), neuronal differentiation 1

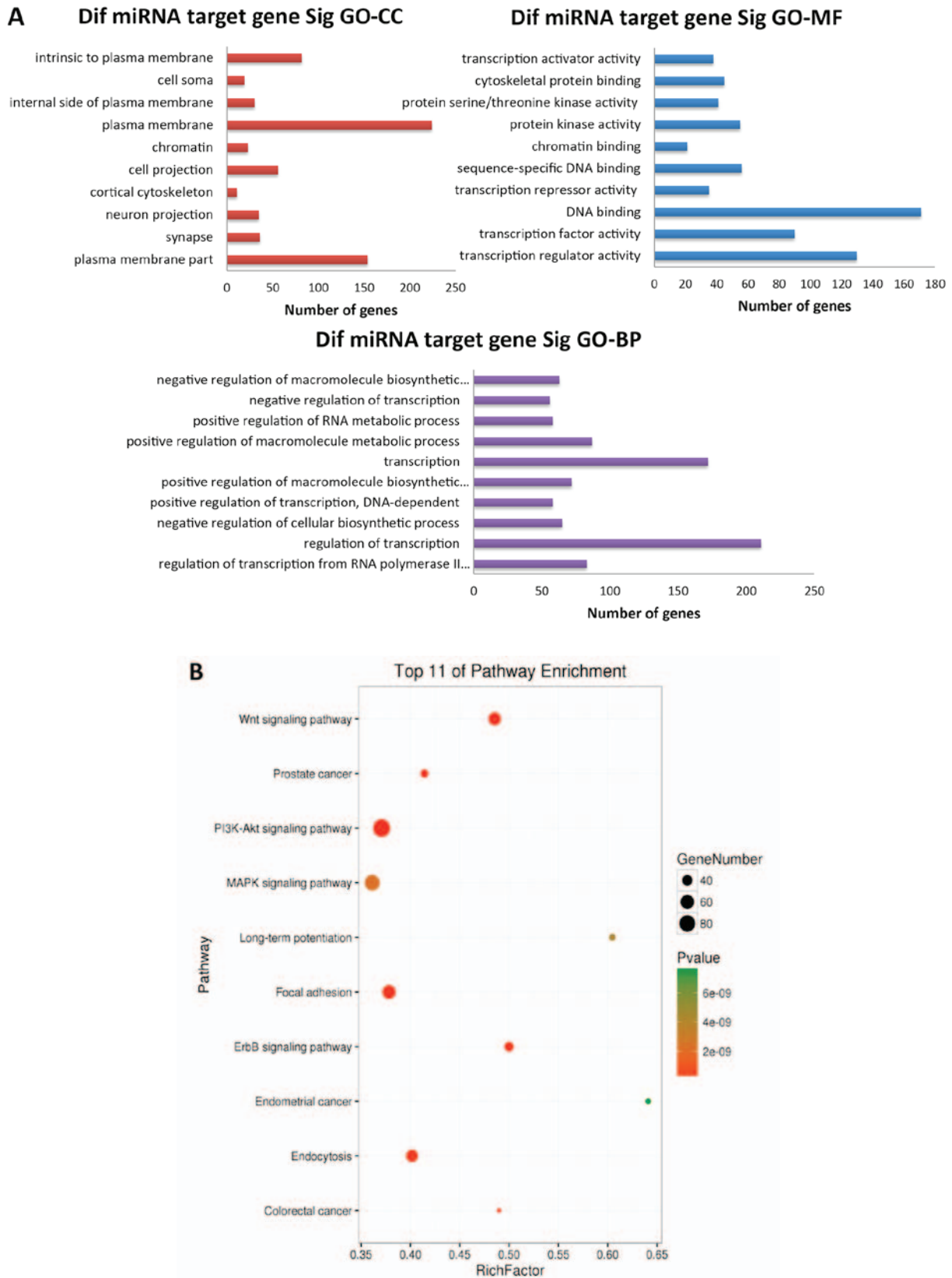


Figure 5. GO and KEGG pathway analyses of differentially expressed miRNAs. (A) The three GO classifications, namely, MF, BP and CC, were evaluated separately and (B) the top 10 significant terms of all KEGG pathways are shown. GO, Gene Ontology; KEGG, Kyoto Encyclopedia of Genes and Genomes; miRNA, microRNA; MF, molecular function; BP, biological process; CC, cellular component; Sig, significant; Dif, differentially expressed.

(NEUROD1) and activated leukocyte cell adhesion molecule (ALCAM) had more interaction with the miRNAs, and RT-qPCR confirmed that these 3 genes were upregulated

in CECs compared with that in SESC (Fig. 4B). DOCK9, NEUROD1 and ALCAM may thus serve an important role in CEC homeostasis and in SESC to CEC transdifferentiation.

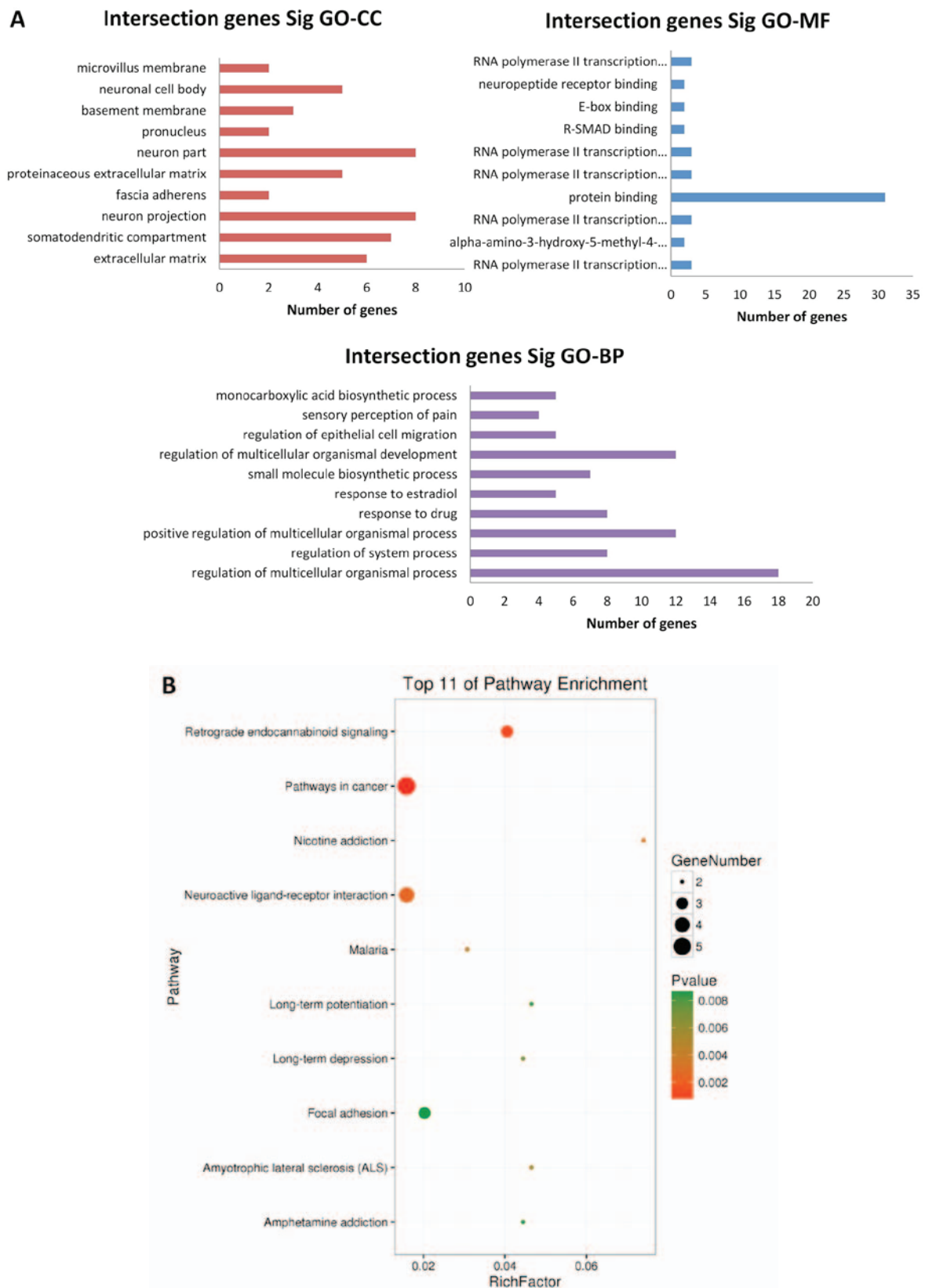


Figure 6. GO and KEGG pathway analyses of intersection genes. (A) The three GO classifications, namely MF, BP and CC, were separately evaluated and (B) the 10 most significant terms of all KEGG pathways are shown. GO, Gene Ontology; KEGG, Kyoto Encyclopedia of Genes and Genomes; miRNA, microRNA; MF, molecular function; BP, biological process; CC, cellular component; Sig, significant; Dif, differentially expressed.

Discussion

The present study elucidated a coordinated miRNA/mRNA

expression profile for SESC and CECs. miRNAs, although non-coding, play a critical role by binding to the 3'-untranslated region (3'UTR) of target genes for post-transcriptional

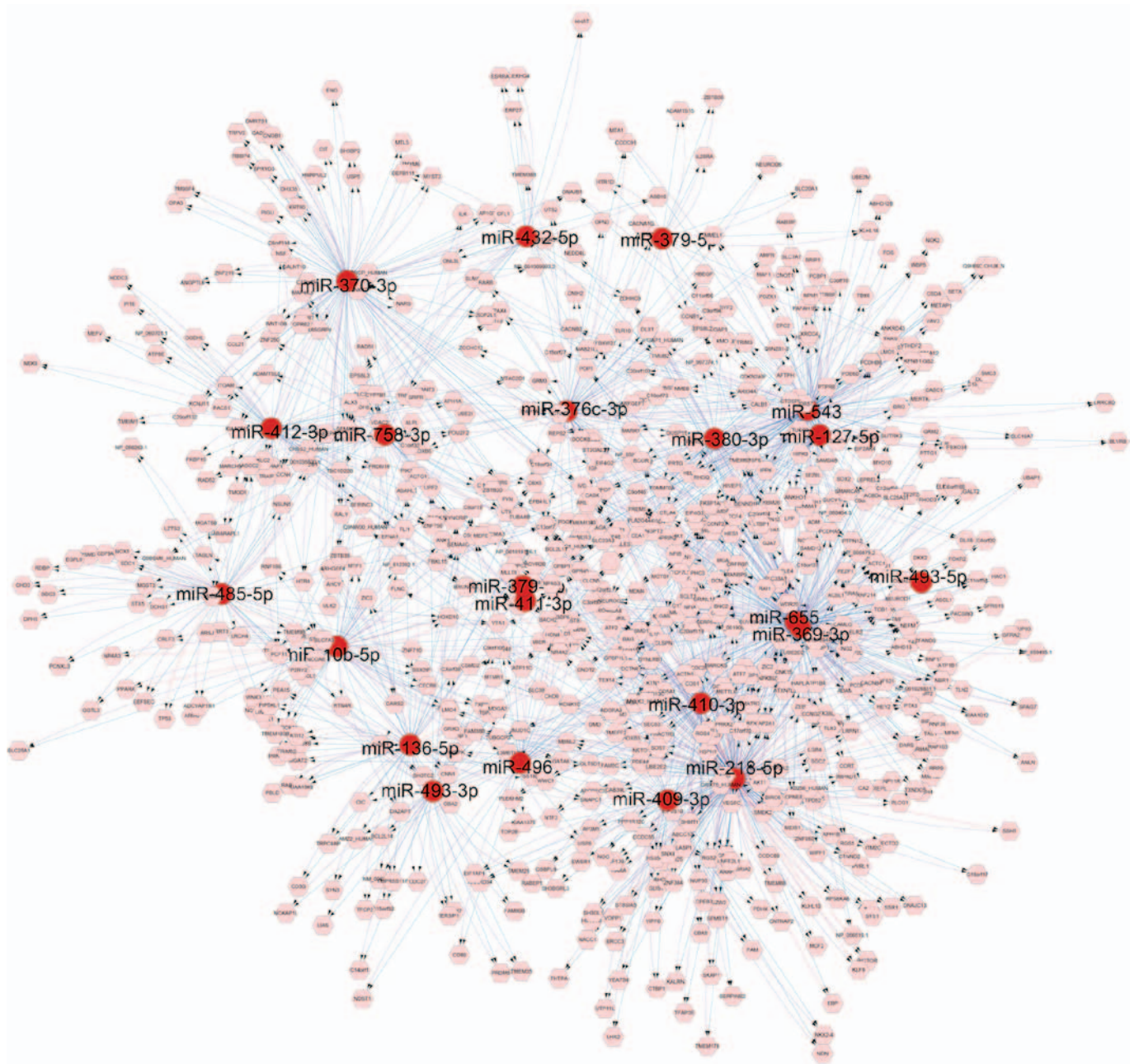


Figure 7. Regulatory network of the differentially expressed miRNAs. The nodes of miRNAs are colored in red and targets are in pink. The edges are colored based on the RegIN source, red and blue for miRTarBase and microCosm, and purple for TargetScan. miR/miRNA, microRNA.

regulation (27). When the expression profile of miRNAs was analyzed in the present study, it was found that miR-10b exhibited the greatest decrease in expression in SESC compared with that in CECs (Figs. 3 and 4A). miR-10b is considered as a marker of cell pathological transformation, particularly the transformation and migration of malignant tumors (28). A growing number of studies have indicated that miR-10b expression is markedly increased in malignant tumors, including breast cancer (29), pancreatic cancer (30), esophageal cancer (31) and glioblastoma (32). Thus, miR-10b may serve a critical role in cell pathological transformation, and is considered as a target for cancer therapy of, for example, breast cancer and neurofibromatosis (33,34). In pathological conditions, CECs convert into skin-like epithelial cells, which in turn may lead to a loss in corneal transparency (2,3);

however, the underlying mechanism remains largely unknown. In this process, the expression of paired box protein Pax-6 (PAX6), a critical transcription factor during eye development, is markedly decreased (3). Analysis of the 3'UTR region of PAX6 indicated that this gene is one of the potential targets of miR-10b (data not shown), and as a tumor suppressor, is suppressed by miR-10b in gliomagenesis (35). Thus, miR-10b may serve an important role in homeostasis and the pathogenesis of CECs through the suppression of PAX6 expression.

KEGG analysis indicated that the Wnt signaling pathway is one of the most significant pathways involved in the differential expression of miRNA target genes. SESC and limbal stem cells originate from the basal layer of embryonic skin (17,18), which develops into different cell types in response to different micro-environments. The Wnt signal has emerged as the predominant

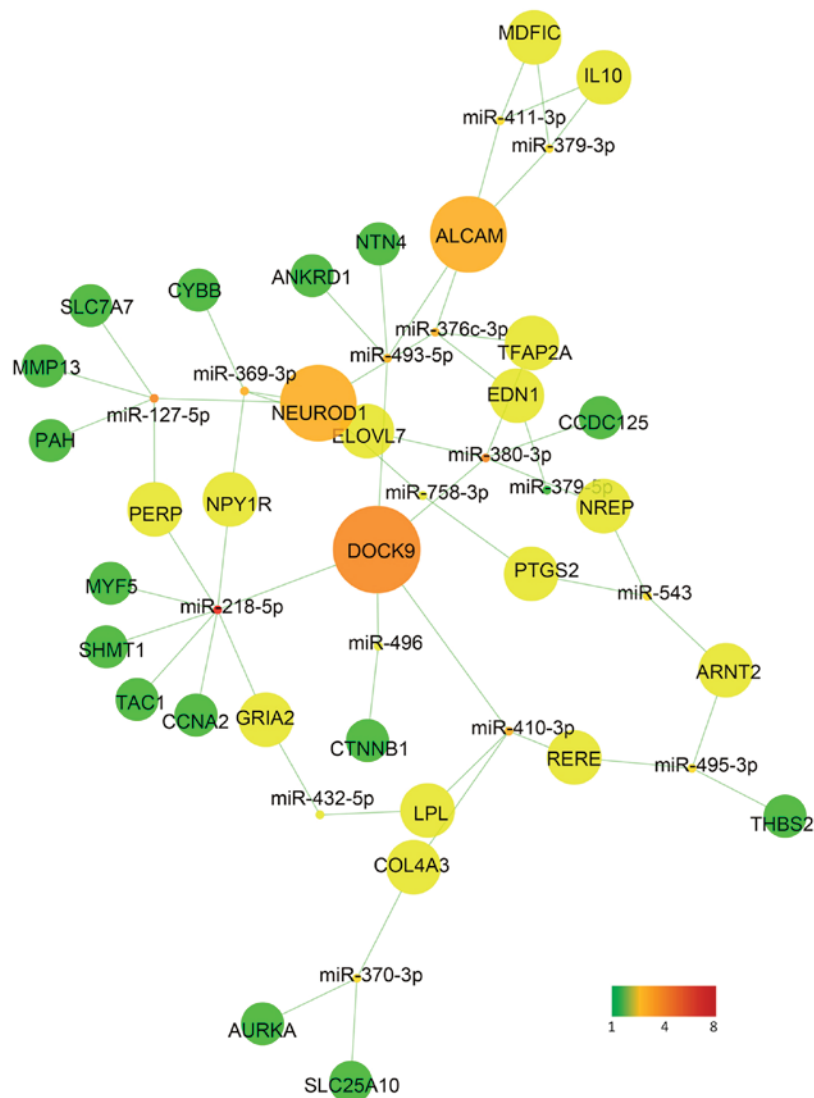


Figure 8. Interaction network of differentially expressed miRNAs and genes. The size of the circle is associated with the numbers of miRNAs that interaction genes interacted with. miR/miRNA, microRNA; DOCK9, dedicator of cytokinesis 9; NEUROD1, neuronal differentiation 1; ALCAM, activated leukocyte cell adhesion molecule.

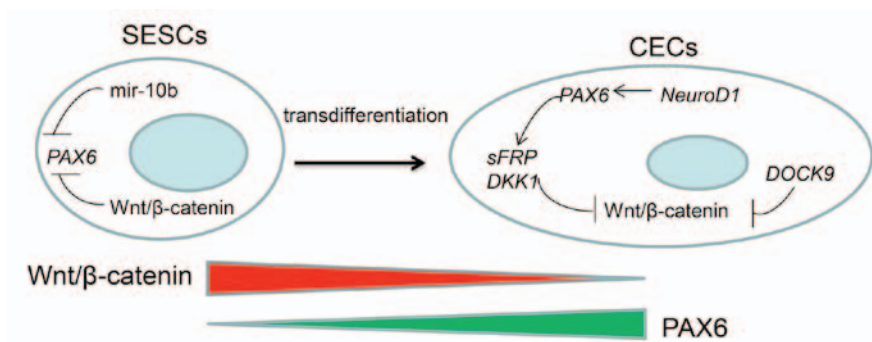


Figure 9. Schematic representation of the putative mechanism involved in the transdifferentiation from SENCs to CECs. The homeostasis of CECs is maintained by stabilized high PAX6 expression, which can inhibit the Wnt/β-catenin signaling pathway. The inhibitory effect of PAX6 may be enhanced by NEUROD1 and DOCK9. In SENCs, the expression of PAX6 is inhibited by miR-10b and the Wnt/β-catenin signaling pathway together. PAX6, miR-10b and the Wnt/β-catenin signaling pathway are the critical factors that predominate the transdifferentiate process. CECs, corneal epithelial cells; SENCs, skin epidermal stem cells; DOCK9, dedicator of cytokinesis 9; NEUROD1, neuronal differentiation 1; miR/miRNA, microRNA; PAX6, paired box protein Pax-6; DKK2, Dickkopf-related protein 2; sFRP, secreted frizzled-related protein.

pathway in the dermal condensation message that determines whether the basal layer of embryonic skin should differentiate

into skin and its appendages (36), as well as subsequently controlling the function of differentiated skin cells (37). CECs

transdifferentiate into skin-like epithelial cells when situated in a pathological condition or induced by dermal developmental signals (2,38). The expression level of β -catenin then sharply increases, indicating that the Wnt signaling pathway has been activated (2,38). Moreover, knockdown of the Wnt signaling inhibitor dickkopf-related protein 2 promotes the differentiation of the corneal epithelia into skin-like epithelial cells and the development of appendages such as hair follicles (39). Thus, the Wnt signaling pathway triggers the pathological transdifferentiation of corneal epithelia into skin-like epithelia and the development, formation and maintenance of the corneal epithelium, which is required to inhibit Wnt signals. It is also possible that the inhibition of a Wnt signal promotes the transdifferentiation of SESCOs into CECs.

The present study found 3 intersection genes, DOCK9, NEUROD1 and ALCAM, which had more interactions with miRNAs. DOCK9 (OMIM 607325) encodes a DOCK protein family member that has GTP/GDP exchange factor activity and specifically activates G-protein cell division control protein 42 homolog (40). Furthermore, it has been reported as the most functionally significant gene for keratoconus (41). DOCK3, one of the members of the DOCK protein family, was found as a negative regulator of Wnt signaling, as it inhibited the nuclear expression of β -catenin (42). Therefore, DOCK9 may play a role in corneal epithelium homeostasis by inhibiting Wnt signaling. NEUROD1 is a member of the NeuroD family of basic helix-loop-helix transcription factors and activates the transcription of genes that contain a specific DNA sequence known as the E-box (43,44). There is evidence that PAX6, a critical transcription factor that defines corneal epithelium homeostasis and pathogenesis (2), is activated by NeuroD1 by binding the E-box in the PAX6 promoter (44). The present study found that NeuroD1 was upregulated in CECs, and thus may act as the upstream activator of PAX6 and maintain the characteristics of corneal epithelia. ALCAM, also known as cluster of differentiation (CD)166, serves an important role in mediating adhesion interactions in epithelial cells. In CD166-deficient cells, mRNA expression of the epithelial-mesenchymal transition (EMT) activator zinc finger E-box-binding homeobox 1 is overexpressed (45), which implies that CD166 deficiency may cause EMT in epithelial cells. MET is one of the pathological changes when homeostasis of the corneal epithelia is disturbed by infection, injury, epithelial hypertrophy or stem cell deficiency (46). Thus, ALCAM may maintain the homeostasis of corneal epithelium by regulating adhesion interactions in corneal epithelial cells. In conclusion, DOCK9, NEUROD1 and ALCAM, which are upregulated in CECs, may serve an important role in maintaining the homeostasis of corneal epithelia, and their overexpression induces the transdifferentiation of SESCOs into corneal epithelial cells.

In conclusion (Fig. 9), the homeostasis of CECs is maintained by the sustained upregulation of PAX6, which can inhibit the Wnt/ β -catenin signaling pathway, and this dermal condensation message causes epidermal changes in the CECs. The inhibitory effect of PAX6 may be enhanced by NEUROD1 and DOCK9. In SESCOs, the expression of PAX6 is inhibited by miR-10b and the Wnt/ β -catenin signaling pathway. Therefore, the transdifferentiation from SESCOs to CECs may be realized by the following approach: i) Forced expression of PAX6 in SESCOs; this approach has previously been demonstrated to

be feasible (2). ii) Forced expression of DOCK9, NEUROD1, and ALCAM. iii) Inhibition of miR-10b expression in SESCOs. iv) Inhibition of the Wnt/ β -catenin signaling pathway in SESCOs. PAX6, miR-10b and the Wnt/ β -catenin signaling pathway are the critical factors that predominate the transdifferentiation process.

The present study investigated the miRNA and mRNA expression profiles of sheep SESCOs and CECs. Coordinated miRNA/mRNA expression analysis revealed that miR-10b, DOCK9, NEUROD1 and the Wnt/ β -catenin signaling pathway may be critical factors in the construction of a regulatory network to regulate corneal homeostasis and transdifferentiation from SESCOs to CECs.

Acknowledgements

This study was supported by grants from the National Natural Science Foundation of China (nos. 31240089 and 31701121) and the Key Project of Higher Education Institutions in Henan Province (nos. 15A180008 and 16A180009).

References

- Pellegrini G, Traverso CE, Franzi AT, Zingirian M, Cancedda R and De Luca M: Long-term restoration of damaged corneal surfaces with autologous cultivated corneal epithelium. *Lancet* 349: 990-993, 1997.
- Ouyang H, Xue Y, Lin Y, Zhang X, Xi L, Patel S, Cai H, Luo J, Zhang M, Zhang M, *et al*: WNT7A and PAX6 define corneal epithelium homeostasis and pathogenesis. *Nature* 511: 358-361, 2014.
- Li W, Chen YT, Hayashida Y, Blanco G, Kheirkah A, He H, Chen SY, Liu CY and Tseng SC: Down-regulation of Pax6 is associated with abnormal differentiation of corneal epithelial cells in severe ocular surface diseases. *J Pathol* 214: 114-122, 2008.
- Lamm V, Hara H, Mammen A, Dhaliwal D and Cooper DK: Corneal blindness and xenotransplantation. *Xenotransplantation* 21: 99-114, 2014.
- Yang X, Moldovan NI, Zhao Q, Mi S, Zhou Z, Chen D, Gao Z, Tong D and Dou Z: Reconstruction of damaged cornea by autologous transplantation of epidermal adult stem cells. *Mol Vis* 14: 1064-1070, 2008.
- Shortt AJ, Secker GA, Notara MD, Limb GA, Khaw PT, Tuft SJ and Daniels JT: Transplantation of ex vivo cultured limbal epithelial stem cells: A review of techniques and clinical results. *Surv Ophthalmol* 52: 483-502, 2007.
- Tseng SC, Prabhasawat P, Barton K, Gray T and Meller D: Amniotic membrane transplantation with or without limbal allografts for corneal surface reconstruction in patients with limbal stem cell deficiency. *Arch Ophthalmol* 116: 431-441, 1998.
- Nakamura T and Kinoshita S: Ocular surface reconstruction using cultivated mucosal epithelial stem cells. *Cornea* 22 (Suppl 7): S75-S80, 2003.
- Utheim TP, Utheim OA, Khan QE and Sehic A: Culture of oral mucosal epithelial cells for the purpose of treating limbal stem cell deficiency. *J Funct Biomater* 7: 5, 2016.
- Nishida K, Yamato M, Hayashida Y, Watanabe K, Yamamoto K, Adachi E, Nagai S, Kikuchi A, Maeda N, Watanabe H, *et al*: Corneal reconstruction with tissue-engineered cell sheets composed of autologous oral mucosal epithelium. *N Engl J Med* 351: 1187-1196, 2004.
- Katikireddy KR, Dana R and Jurkunas UV: Differentiation potential of limbal fibroblasts and bone marrow mesenchymal stem cells to corneal epithelial cells. *Stem Cells* 32: 717-729, 2014.
- Gu S, Xing C, Han J, Tso MO and Hong J: Differentiation of rabbit bone marrow mesenchymal stem cells into corneal epithelial cells in vivo and ex vivo. *Mol Vis* 15: 99-107, 2009.
- Ahmad S, Stewart R, Yung S, Kolli S, Armstrong L, Stojkovic M, Figueiredo F and Lako M: Differentiation of human embryonic stem cells into corneal epithelial-like cells by in vitro replication of the corneal epithelial stem cell niche. *Stem Cells* 25: 1145-1155, 2007.

14. Gomes JA, Geraldes Monteiro B, Melo GB, Smith RL, Cavenaghi Pereira da Silva M, Lizier NF, Kerkis A, Cerruti H and Kerkis I: Corneal reconstruction with tissue-engineered cell sheets composed of human immature dental pulp stem cells. *Invest Ophthalmol Vis Sci* 51: 1408-1414, 2010.
15. Toma JG, Akhavan M, Fernandes KJ, Barnabé-Heider F, Sadikot A, Kaplan DR and Miller FD: Isolation of multipotent adult stem cells from the dermis of mammalian skin. *Nat Cell Biol* 3: 778-784, 2001.
16. Dyce PW, Wen L and Li J: In vitro germline potential of stem cells derived from fetal porcine skin. *Nat Cell Biol* 8: 384-390, 2006.
17. Chee KY, Kicic A and Wiffen SJ: Limbal stem cells: The search for a marker. *Clin Experiment Ophthalmol* 34: 64-73, 2006.
18. Lavker RM and Sun TT: Epidermal stem cells: Properties, markers, and location. *Proc Natl Acad Sci USA* 97: 13473-13475, 2000.
19. Bose A, Teh MT, Mackenzie IC and Waseem A: Keratin k15 as a biomarker of epidermal stem cells. *Int J Mol Sci* 14: 19385-19398, 2013.
20. Forni MF, Trombetta-Lima M and Sogayar MC: Stem cells in embryonic skin development. *Biol Res* 45: 215-222, 2012.
21. Ghadially R: 25 years of epidermal stem cell research. *J Invest Dermatol* 132: 797-810, 2012.
22. Blazejewska EA, Schlötzer-Schrehardt U, Zenkel M, Bachmann B, Chankiewicz E, Jacobi C and Kruse FE: Corneal limbal microenvironment can induce transdifferentiation of hair follicle stem cells into corneal epithelial-like cells. *Stem Cells* 27: 642-652, 2009.
23. Saichanma S, Bunyaratvej A and Sila-Asna M: In vitro transdifferentiation of corneal epithelial-like cells from human skin-derived precursor cells. *Int J Ophthalmol* 5: 158-163, 2012.
24. Araki K, Ohashi Y, Sasabe T, Kinoshita S, Hayashi K, Yang XZ, Hosaka Y, Aizawa S and Handa H: Immortalization of rabbit corneal epithelial cells by a recombinant SV40-adenovirus vector. *Invest Ophthalmol Vis Sci* 34: 2665-2671, 1993.
25. Yang X, Qu L, Wang X, Zhao M, Li W, Hua J, Shi M, Moldovan N, Wang H and Dou Z: Plasticity of epidermal adult stem cells derived from adult goat ear skin. *Mol Reprod Dev* 74: 386-396, 2007.
26. Livak KJ and Schmittgen TD: Analysis of relative gene expression data using real-time quantitative PCR and the 2^{-Delta Delta} C(T) Method. *Methods* 25: 402-408, 2001.
27. Shukla GC, Singh J and Barik S: MicroRNAs: Processing, maturation, target recognition and regulatory functions. *Mol Cell Pharmacol* 3: 83-92, 2011.
28. Baffa R, Fassan M, Volinia S, O'Hara B, Liu CG, Palazzo JP, Gardiman M, Rugge M, Gomella LG, Croce CM, *et al*: MicroRNA expression profiling of human metastatic cancers identifies cancer gene targets. *J Pathol* 219: 214-221, 2009.
29. Ma L, Teruya-Feldstein J and Weinberg RA: Tumour invasion and metastasis initiated by microRNA-10b in breast cancer. *Nature* 449: 682-688, 2007.
30. Bloomston M, Frankel WL, Petrocca F, Volinia S, Alder H, Hagan JP, Liu CG, Bhatt D, Taccioli C and Croce CM: MicroRNA expression patterns to differentiate pancreatic adenocarcinoma from normal pancreas and chronic pancreatitis. *JAMA* 297: 1901-1908, 2007.
31. Tian Y, Luo A, Cai Y, Su Q, Ding F, Chen H and Liu Z: MicroRNA-10b promotes migration and invasion through KLF4 in human esophageal cancer cell lines. *J Biol Chem* 285: 7986-7994, 2010.
32. Ciafrè SA, Galardi S, Mangiola A, Ferracin M, Liu CG, Sabatino G, Negrini M, Maira G, Croce CM and Farace MG: Extensive modulation of a set of microRNAs in primary glioblastoma. *Biochem Biophys Res Commun* 334: 1351-1358, 2005.
33. Ma L, Reinhardt F, Pan E, Soutschek J, Bhat B, Marcusson EG, Teruya-Feldstein J, Bell GW and Weinberg RA: Therapeutic silencing of miR-10b inhibits metastasis in a mouse mammary tumor model. *Nat Biotechnol* 28: 341-347, 2010.
34. Chai G, Liu N, Ma J, Li H, Oblinger JL, Prahalad AK, Gong M, Chang LS, Wallace M, Muir D, *et al*: MicroRNA-10b regulates tumorigenesis in neurofibromatosis type 1. *Cancer Sci* 101: 1997-2004, 2010.
35. Lin J, Teo S, Lam DH, Jeyaseelan K and Wang S: MicroRNA-10b pleiotropically regulates invasion, angiogenicity and apoptosis of tumor cells resembling mesenchymal subtype of glioblastoma multiforme. *Cell Death Dis* 3: e398, 2012.
36. Widelitz RB: Wnt signaling in skin organogenesis. *Organogenesis* 4: 123-133, 2008.
37. Lim X and Nusse R: Wnt signaling in skin development, homeostasis, and disease. *Cold Spring Harb Perspect Biol* 5: 5, 2013.
38. Pearton DJ, Yang Y and Dhoulailly D: Transdifferentiation of corneal epithelium into epidermis occurs by means of a multistep process triggered by dermal developmental signals. *Proc Natl Acad Sci USA* 102: 3714-3719, 2005.
39. Mukhopadhyay M, Gorivodsky M, Shtrom S, Grinberg A, Niehrs C, Morasso MI and Westphal H: Dkk2 plays an essential role in the corneal fate of the ocular surface epithelium. *Development* 133: 2149-2154, 2006.
40. Kwofie MA and Skowronski J: Specific recognition of Rac2 and Cdc42 by DOCK2 and DOCK9 guanine nucleotide exchange factors. *J Biol Chem* 283: 3088-3096, 2008.
41. Czugala M, Karolak JA, Nowak DM, Polakowski P, Pitarque J, Molinari A, Rydzanicz M, Bejjani BA, Yue BY, Szaflik JP, *et al*: Novel mutation and three other sequence variants segregating with phenotype at keratoconus 13q32 susceptibility locus. *Eur J Hum Genet* 20: 389-397, 2012.
42. Caspi E and Rosin-Arbesfeld R: A novel functional screen in human cells identifies MOCA as a negative regulator of Wnt signaling. *Mol Biol Cell* 19: 4660-4674, 2008.
43. Poulin G, Turgeon B and Drouin J: NeuroD1/beta2 contributes to cell-specific transcription of the proopiomelanocortin gene. *Mol Cell Biol* 17: 6673-6682, 1997.
44. Marsich E, Vetere A, Di Piazza M, Tell G and Paoletti S: The PAX6 gene is activated by the basic helix-loop-helix transcription factor NeuroD/BETA2. *Biochem J* 376: 707-715, 2003.
45. Fujiwara K, Ohuchida K, Sada M, Horioka K, Ulrich CD III, Shindo K, Ohtsuka T, Takahata S, Mizumoto K, Oda Y, *et al*: CD166/ALCAM expression is characteristic of tumorigenicity and invasive and migratory activities of pancreatic cancer cells. *PLoS One* 9: e107247, 2014.
46. Park GB, Kim D, Kim YS, Kim S, Lee HK, Yang JW and Hur DY: The Epstein-Barr virus causes epithelial-mesenchymal transition in human corneal epithelial cells via Syk/src and Akt/Erk signaling pathways. *Invest Ophthalmol Vis Sci* 55: 1770-1779, 2014.



This work is licensed under a Creative Commons Attribution-NonCommercial-NoDerivatives 4.0 International (CC BY-NC-ND 4.0) License.